

Large Eddy Simulation of Flowfield around Marine Propeller on Unstructured Meshes

Zhen-yu Huang, Xi-zhong Wei and Fang-wen Hong

China Ship Scientific Research Center(CSSRC), Wuxi, China

ABSTRACT The cell-centered finite volume method (FVM) on unstructured meshes is applied to the large eddy simulation (LES) of viscous flowfield around marine propellers. Based on gradient reconstruction by the weighted least square method, the inviscid fluxes are interpolated with a third-order unstructured MUCSL-scheme and the viscous fluxes are calculated with the directional derivative method. Numerical results of hydrodynamic force, pressure on the blades and velocity in the wake of propeller are in good agreement with the experimental data.

KEYWORD: Large Eddy Simulation (LES), Finite Volume Method (FVM), Unstructured Mesh, Propeller

1 INTRODUCTION

Numerical methods are widely used in the simulation of viscous flow around marine propellers, which can provide hydrodynamic performance, pressure distribution on the blades and some details of flow structure around propellers such as separation and reattachment in boundary layer, leading- or trailing-edge and tip vortices etc. Usually propellers' inflow is induced by the ship hull, shaft, rudder and various appendages, which is unsteady and non-uniform. The unsteady and non-uniform inflow leads blade vibration, cavitation, erosion and produce hydro-noise. The numerical prediction of unsteady force, hydro-noise and cavitation of propellers in a non-uniform wake is still a challenge to the computation fluid dynamics(CFD) even at the beginning of 21st century.

Since 1980's, numerical methods for RANS equation have been applied to the prediction of propellers' hydrodynamic performance and flow structure of propeller-hull interaction. Open-water characteristics, pressure distributions and streamlines on the blade, circumferential-mean velocity around propeller are very close to the experimental data, RANS calculation can give some details of flow structure, e.g. separation and reattachment of boundary layer, tip vortices. However RANS remains aside from the inherent limitation of Reynolds-averaging in capturing details of such transient events like unsteady force and pressure fluctuation of the blade with an acceptable accuracy now. In that regard, Large Eddy Simulation has been considered having merits, inasmuch as at least large scale turbulent structures are directly resolved, which is further justifiable for the unsteady flow around propellers operated at the stern of ships. Unfortunately, LES requires a far greater amount of computational resource than RANS-based approach. Moreover, LES still needs models for subgrid-scale turbulence.

Apparently, it is the challenge to develop a suitable SGS model for the unsteady flow and for the two-phase cavitation flows about propellers.

Most of researchers apply Reynolds-averaged Navier-Stokes (RANS) equations with the closure of various turbulence models to simulate the flowfields around the propellers, the hull and interaction between hull and propeller, they have got some very good results, such as drag, pressure and velocity distribution [Chen 1998, Oh 1992, Stern 1988, Stern 1992, Stern 1994, Tang 1998, Uto 1992]. Several authors apply LES to viscous flow about ships and submarines [Bensaw 2004, Lillberg 2004, Huang 2006A]. Martin [2006] and Bensow [2006] apply to the propeller crashback and propeller-hull interaction, they obtain very accurate temporal-mean hydrodynamic performance and parts of vortices structure in the complex flow.

In this paper, a LES computer code based on cell-centered finite volume method (FVM) on unstructured meshes has been developed and applied to viscous flow field around propeller DTRC P4119, the result is in good agreement with the experiment data, which will gain some numerical experience to apply LES method in the prediction of propeller unsteady force, cavitations and hydro-noise of propeller in non-uniform flow.

2 GOVERNING EQUATIONS

The weakly compressible flow around the non-cavitating marine propeller can be treated as incompressible flow, which is governed by incompressible Navier-Stokes equation and the equation of continuity. In this paper, the artificial compressibility method, which adds a pseudo time-derivative of the pressure to the continuity equation, is used to couple the equations of motion with the equation of continuity. Then most of efficient implicit time-dependant methods in computational aerodynamics can be applied to solve viscous incompressible flow [Chorin 1967].

The governing equations in the form of absolute flow in far field are formulated in a reference frame rotating with angular velocity of marine propeller, which allows more accurate calculations of the fluxes in the finite-volume method (FVM) and obtains accurate solutions on nonuniform unstructured grids [Agarwal 1987, Chen 1991].

Let the reference frame is rotating with a uniform angular velocity ω about the x axis, (u, v, w) , $(u_0, v_0, w_0) = (0, \omega z, -\omega y)$ are absolute and relative velocity. The governing equations are written as:

$$\frac{\partial Q}{\partial \tau} + \frac{\partial(E - E_v)}{\partial x} + \frac{\partial(F - F_v)}{\partial y} + \frac{\partial(G - G_v)}{\partial z} = H \quad (1)$$

Where:

$$Q = (p, u, v, w)^T$$

$$E = (\beta \hat{u}, u \hat{u} + p, v \hat{u}, w \hat{u})^T$$

$$F = (\beta \hat{v}, u \hat{v}, v \hat{v} + p, w \hat{v})^T$$

$$G = (\beta \hat{w}, u \hat{w}, v \hat{w}, w \hat{w} + p)^T$$

$$(\hat{u}, \hat{v}, \hat{w}) = (u - u_0, v - v_0, w - w_0)$$

The source term $H = (0, 0, \varpi w, -\varpi v)^T$ is the rotating force generated by propellers, E_v , F_v , G_v are the viscous fluxes.

By using spatial filter with the control volume, the equation of large eddy simulation (LES) are reached. And the simple Smagorinsky's [Smagorinsky 1963] subgrid scale model (SGS) is introduced to close the subgrid stress in the filtered equations, which can be written as:

$$\tau_{ij} = \overline{u_i u_j} - \overline{u_i} \overline{u_j} = 2(C_s L)^2 |\overline{S}_{ij}| \overline{S}_{ij} - \frac{1}{3} \tau_{kk} \delta_{ij} \quad (2)$$

The length scale is geometric mean of the grid spacing $L = V^{1/3}$ (V is the cell volume) and turbulent viscosity is defined.

$$\nu_t = (C_s L)^2 |\overline{S}_{ij}| \quad (3)$$

Where

$$\overline{S}_{ij} = \frac{1}{2} \left(\frac{\partial \overline{u}_i}{\partial x_j} + \frac{\partial \overline{u}_j}{\partial x_i} \right) \quad (4)$$

$$|\overline{S}_{ij}| = \sqrt{2 \overline{S}_{ij} \overline{S}_{ij}}$$

The SGS model coefficient $C_s = 0.065 \sim 0.2$. In order to reduce the number of grids near the wall and to save the computing time, the log-law wall function [Xu 1989, Huang 2006A] is applied to get the friction velocity and turbulent viscosity at the first point near the wall.

3 NUMERICAL METHOD

By using the finite volume method (FVM), governing equations (Eqs. 1) are integrated over the control volume V . Let $\hat{E} = E\vec{i} + F\vec{j} + G\vec{k}$, $\hat{E}_v = E_v\vec{i} + F_v\vec{j} + G_v\vec{k}$, with the use of the divergence theorem, the semi-discrete form of governing equations can be written as

$$V \frac{\partial Q}{\partial \tau} + \sum_{j \in N(i)} (\hat{E}_{ij} - \hat{E}_{vij}) \cdot \vec{n}_{ij} S_{ij} = V \cdot H \quad (5)$$

S_{ij} is area and \vec{n}_{ij} is the unit outward normal vector of the j th surface surround the control volume, \hat{E}_{ij} and \hat{E}_{vij} are the convective and viscous flux, respectively. The convective flux is evaluated with Roe's scheme [Roe 1981].

$$E_{ij} = \frac{1}{2} [E(Q_{ij}^L, \vec{n}_{ij}) + E(Q_{ij}^R, \vec{n}_{ij}) - |\overline{A}| (Q_{ij}^R - Q_{ij}^L)] \quad (6)$$

Where, \overline{A} is the Jacobian matrix of the inviscid flux.

$$|\overline{A}| = \left| \frac{\partial \hat{E}}{\partial Q} \right| = R |\Lambda| L \quad (7)$$

Λ is the diagonal matrix of eigenvalue, and R_i , L_i are right and left eigenvector matrices of Λ , The variables U_{ij}^L , U_{ij}^R in equation (6) are interpolated by using unstructured MUSCL scheme (U-MUSCL)[Clarence 2005].

$$Q_{ij}^L = Q_i + \frac{\chi}{2}(Q_j - Q_i) + \frac{1-\chi}{2} \nabla Q_i \cdot \vec{r}_{ij} \quad (8)$$

$$Q_{ij}^R = Q_j - \frac{\chi}{2}(Q_j - Q_i) - \frac{1-\chi}{2} \nabla Q_j \cdot \vec{r}_{ij} \quad (9)$$

\vec{r}_{ij} is the directive vector from nodes i to node j, the parameter χ is 0 to 1, which leads to different accurate for U-MUSCL. In this paper, χ is set to 0.5, which leads a third-order variable extrapolation to the control surface. The gradient of the variables ∇Q_i and ∇Q_j are reconstructed with Weighted Least-Squares method.

Several methods are available to discretize the viscous terms. The simplest method is to calculate the gradient of the velocities at each cell center ∇u_i , then average the values at the interface between two cells, but these schemes is not stable and sometime it brings too much numerical diffusion to the solution which may smear the useful details of complicated flows. In this paper, the directional derivative method is applied to discretize the viscous terms, the gradient of the velocities at the interface are split into a normal and a tangent component to the interface[Clarence 2003].

$$\nabla U_{ij} = (\nabla U_{ij})_{\text{norm}} + (\nabla U_{ij})_{\text{tang}} \quad (10)$$

The normal component is approximated by the derivative along the edge.

$$(\nabla \vec{u}_{ij})_{\text{normal}} \approx \frac{\vec{u}_j - \vec{u}_i}{|\vec{r}_{ij}|} \vec{n}_{ij} \quad (11)$$

The tangent component is calculated by

$$(\nabla \vec{u}_{ij})_{\text{tang}} = \overline{\nabla \vec{u}_{ij}} - (\overline{\nabla \vec{u}_{ij}} \cdot \vec{n}_{ij}) \vec{n}_{ij} \quad (12)$$

Where

$$\overline{\nabla u_{ij}} = \frac{\nabla u_i + \nabla u_j}{2} \quad (13)$$

The gradient at the interface can be expressed as

$$\nabla \vec{u}_{ij} = \overline{\nabla \vec{u}_{ij}} + \left(\frac{\vec{u}_j - \vec{u}_i}{|\vec{r}_{ij}|} - \overline{\nabla \vec{u}_{ij}} \cdot \vec{n}_{ij} \right) \vec{n}_{ij} \quad (14)$$

The temporal discretization of governing equations (Eqs.5) generate a series of algebraic equations, which are solved by a full implicit matrix-free method LU-SGS [Yoon 1988, Luo 1998, Luo 2001, Huang 2006B].

4 RESULTS

The above LES solver has been applied to calculate viscous flowfield around 3-blade propeller DTMB P4119 in a uniform flow. The propeller was designed in the 1960's to validate lifting surface methods[ITTC 1998], whose design condition corresponds to an advance coefficient $J=0.833$. The hybrid grid of tetrahedral and hexahedral shape are

filled in the domain about the blade and hub, and the tetrahedral grids is near the blade and hub, the hexahedral grids is far from the blades, the total is about 27,000. Figure 1 shows the grids near the blade and hub in one passage. The geometry modeling and grid generation are finished in Gambit software, then the exported mesh file is read and imported to the LES solver.

The numerical results in Figure 2 shows that K_T and K_Q are in good agreement with the experimental data. The relative error is less than 3% for thrust and 5% for torque. The pressure distributions on the blade derived from velocity in boundary layer are given by Jessup through LDV measurement [Jessup 1998]. The pressure distribution along three radius of the blade are given in Figure 3 under design condition ($J=0.833$), which are nearly same as the experiment data, only besides a little difference near the leading edge due to the bad grid distribution. Figure 4 shows the circumferential-mean velocity in downstream $x=0.3281R$ for $J=0.833$. The variety of velocity in three direction with the phase angle in $x=0.3281R$ plane are given and compared with the experiment data at the position of $r/R=0.7$ (Figure 5). The results agree with the measurements very well except the tangential velocities near the rotating hub. Numerical simulation does not capture the velocity peak in the downstream region of blade boundary layer, maybe because the grids are too coarse in the region. The grid-independence of LES and features of propeller's wake in a non-uniform flow is in the progressing work.

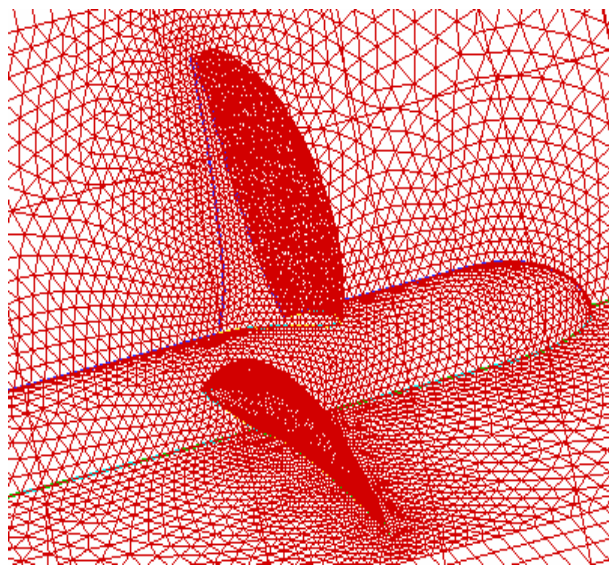


Figure 1 Grids near blade and hub

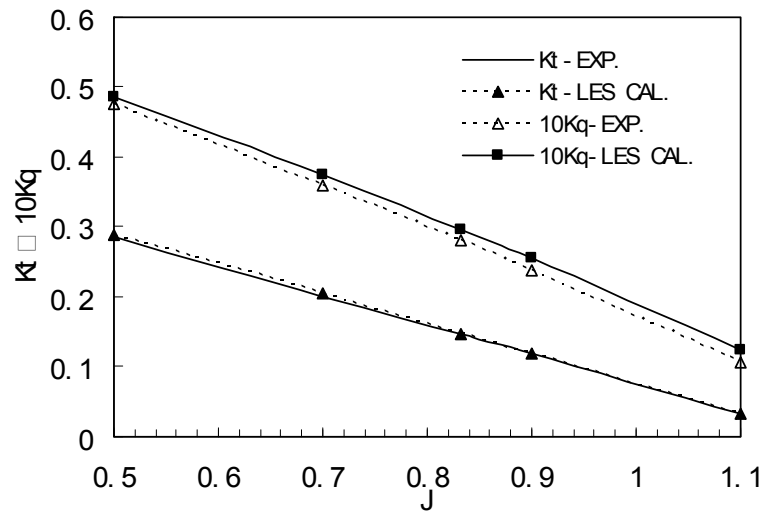


Figure 2 Open water characteristics of P4119

5 CONCLUSION

The viscous flow around the propeller DTRC P4119 is simulated on the hybrid meshes with a LES method. The results of hydrodynamic performance, pressure coefficient on the blade and velocity in the wake are in good agreement with the Jessup's experiment data, which give a good beginning of LES to predict the propeller unsteady force, propeller cavitations and noise in a non-uniform flow.

REFERENCE

- Agarwal R. K. and Deese J. E. 1987, Euler calculations for flowfield of a helicopter rotor in hover, *J. Aircraft*, 24(4): 231-238
- Bensow R. E., Persson T., Fureby C., et al. 2004, Large Eddy Simulation of the Viscous Flow around Submarine Hulls. 25th Symposium on naval Hydrodynamics, Canada
- Chen C. L., Mccroskey W. J., et al 1991, Numerical solutions of forward-flight rotor flow using upwind method, *J. Aircraft*, 28(6): 374-380
- Chen J D, Zhou W X, Tang D H, Dong S T. 1998, Comparative calculations of unsteady propeller performance by panel method. 22nd ITTC Propulsion Committee Propeller RANS/Panel Method Workshop, Grenble
- Chorin A J. 1967, A numerical method for solving incompressible viscous flow problems, *Journal of computational Physics*, Vol.2:275-312
- Clarence O.E.B 2005. Higher order variable extrapolation for unstructured finite volume RANS flow solvers. AIAA Paper 2005-0499
- Clarence O.E.B, Sheng C. H. Sheng, Newman J. C. et al 2003. Verification and Validation of Forces Generated by An Unstructured Flow Solver. AIAA 2003-3983
- Huang Z Y, Miao G P. 2006A, Large Eddy Simulation of Incompressible Viscous Flow past Underwater Configuration, *Journal of Hydrodynamics, Ser. A*, 21(2): 190~197
- Huang Z. Y., Miao G. P. 2006B, A Matrix-free Implicit Method for Incompressible Flow around 3D Complex Underwater Bodies, *Journal of Hydrodynamics, Ser. B*, 18(2):192~198
- ITTC, Propeller RANS/Panel Method Workshop, 1998, 22nd ITTC Propulsion Committee
- Jessup S D. 1998, Experimental data for RANS calculations and comparisons, 22nd ITTC Propulsion Committee, Propeller RANS/Panel Method Workshop
- Lillberg E., Svennberg U. 2004, Large Eddy Simulation of the Viscous Flow around a ship Hull Including the free-surface. 25th Symposium on naval Hydrodynamics, Canada,
- Luo H., Baum J. D. ,Lohner R. 1998. A fast Matrix-Free Implicit Method for compressible flow on unstructured grids. *Journal of computational physics*, 146, 664-690
- Luo H., Baum J. D. ,Lohner R. 2001, An accurate, fast, matrix-free implicit method for computing unsteady flows on unstructured grids. *Computers and Fluids* 30 (2001) 137-159
- Martin V., Krishnan M. 2006, Large Eddy Simulation of crashback in marine propellers. 26th Symposium on Naval Hydrodynamics, Roman, Italy
- Oh K.J., Kang S.H 1992. Numerical Calculation of the Viscous Flow Around a Rotating Marine Propeller. 19th ONR Symposium on Naval Hydrodynamics, Seoul, Korea
- Roe P. L. 1981, Approximate Riemann Solvers, Parameter Vectors, and Difference Scheme, *J. of Comp. Phys.*, 43,357-372
- Smagorinsky J 1963. General circulation experiments with primitive equation. *Monthly Weather Review*, 91-99
- Stern F., Kim H T., Patel V.C. Chen H.C 1988, A viscous-Flow Approach to the Computation of propeller-Hull Interaction. *J.S.R.* 32: 246-284
- Stern F., Patel V.C., Kim H.T, Chen H.C. 1986, Propeller-Hull interaction: A New Approach. 16th Symposium on Naval Hydrodynamics
- Stern F., Zhang D., Chen B., Kim H., Jessup S. 1994, Computing of Viscous Marine Propeller Blade and Wake Flow, 20th Symposium on Naval Hydrodynamics, California.
- Tang D H, Chen J D, Zhou W X. 1998, Comparative calculations of propeller performance by RANS/Panel Method, 22nd ITTC Propulsion Committee Propeller RANS/Panel Method Workshop, Grenble
- Uto S. 1992. Computation of Incompressible Viscous Flow around a Marine Propeller, *J. SNAJ*
- Xu W X, Xu W C.1989, *Viscous Fluid Mechanics*, Beijing Institute of technology Press
- Yoon S. and Jameson A 1988, Lower-Upper Symmetric-Gauss-Seidel Method for the Euler and Navier-Stokes Equations. *AIAA Journal*, 22:1025-1025

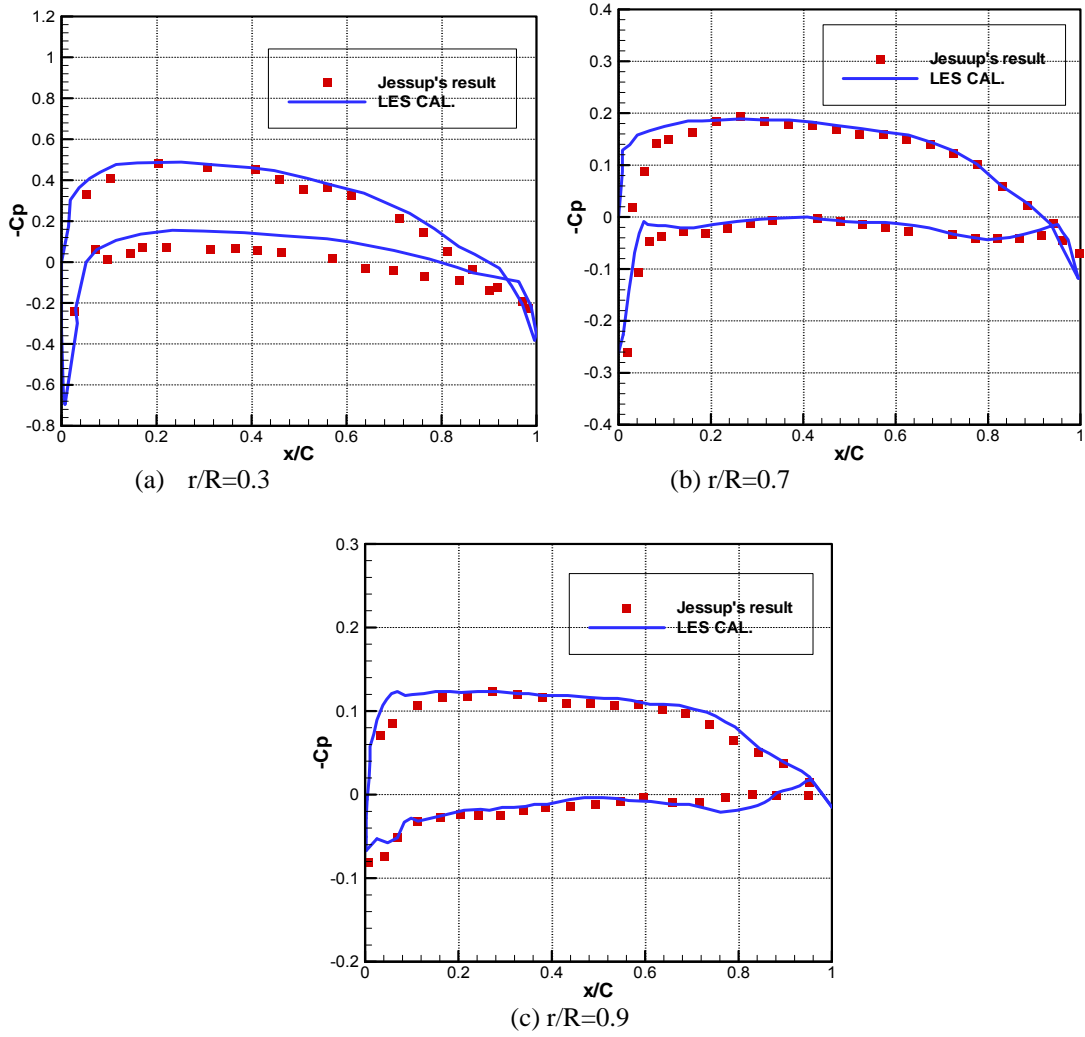
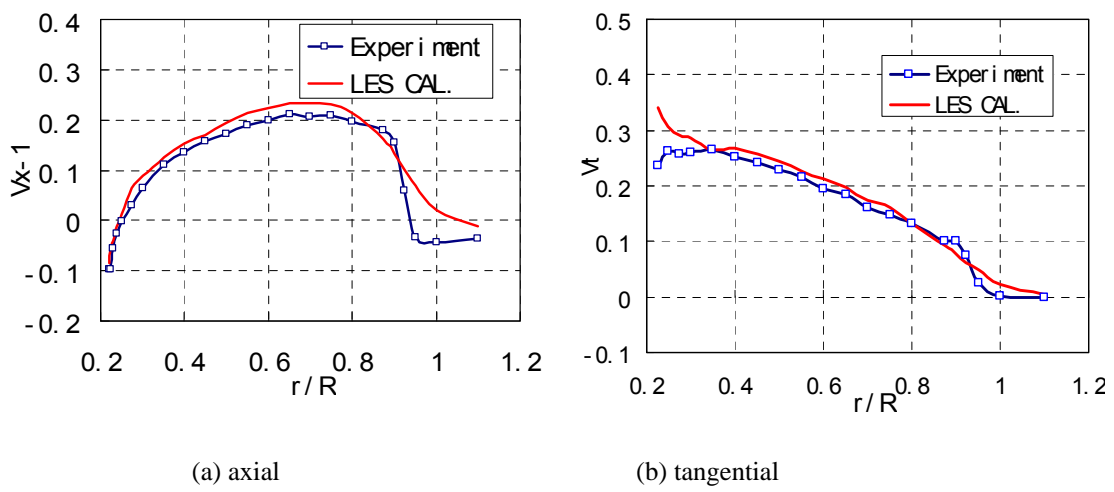
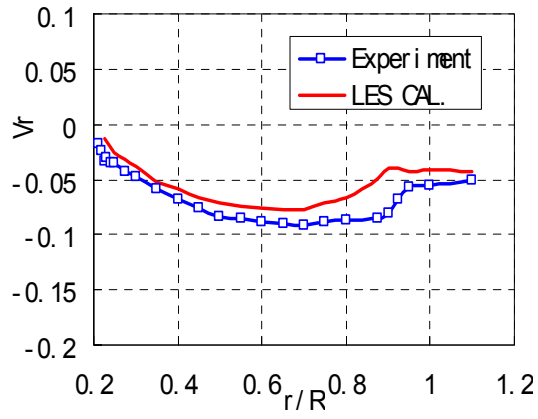


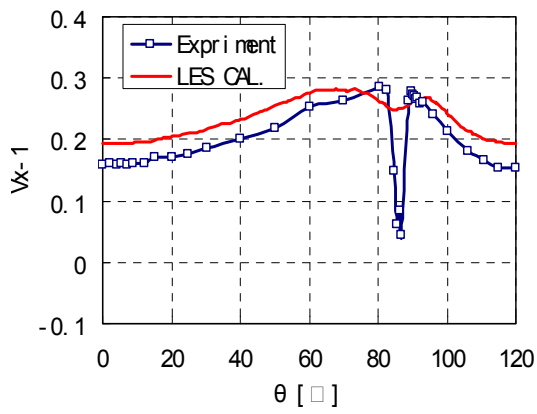
Figure. 3 Comparison of pressure distribution with experiment



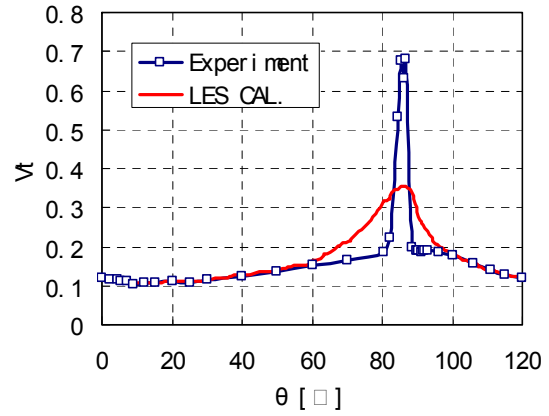


(c) radial

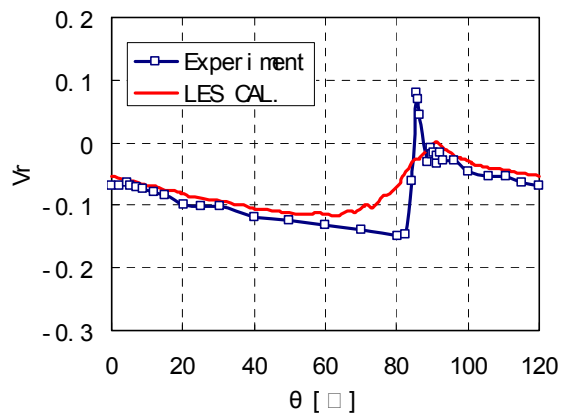
Figure 4 Circumferential-mean velocity downstream at $x = 0.3281R$



(a) axial



(b) tangential



(c) radial

Figure 5 Velocity in one passage of propeller downstream at $x = 0.3281R$ ($r/R = 0.7$)